Am J Cancer Res 2018;8(9):1788-1800
www.ajcr.us /ISSN:2156-6976/ajcr0083101

Original Article

Altered expression pattern of circular RNAs in metastatic oral mucosal melanoma

Houyu Ju[1,2,3*], Liming Zhang[1,2,3*], Lu Mao[1,2,3], Shuli Liu[1,2,3], Weiya Xia[4], Jingzhou Hu[1,2,3], Min Ruan[1,2,3], Guoxin Ren[1,2,3]

[1]Department of Oral Maxillofacial-Head and Neck Oncology, Shanghai Ninth People's Hospital, School of Medicine, Shanghai Jiao Tong University, China; [2]Shanghai Key Laboratory of Stomatology and Shanghai Research Institute of Stomatology, Shanghai, China; [3]National Clinical Research Center of Stomatology, Shanghai, China; [4]Department of Molecular and Cellular Oncology, The University of Texas MD Anderson Cancer Center, Houston, Texas. [*]Co-first authors.

Received July 25, 2018; Accepted August 20, 2018; Epub September 1, 2018; Published September 15, 2018

Abstract: Circular RNAs (circRNAs) are known to be associated with carcinogenesis, and can serve as potential biomarkers for cancer diagnosis and therapeutic implications. However, little is known about their expression patterns in oral mucosal melanoma (OMM), an extremely rare cancer that is distinct from cutaneous melanoma for its clinical course and prognosis. To investigate circRNAs expression profile in OMM, we performed a circRNAs microarray to analyze 6 primary OMM samples with lymph nodes dissemination, and constructed a genome-wide circRNA profile. Our results revealed that 90 circRNAs were significantly dysregulated in the metastatic OMM tissues when compared to the paired adjacent tissues. Among them, hsa_circ_0005320, hsa_circ_0067531, hsa_circ_0008042 were significantly upregulated in primary tumor and metastatic lymph nodes compared to paired adjacent normal tissues and non-metastatic lymph nodes, whereas the expression of hsa_circ_0000869 and hsa_circ_0000853 were downregulated relatively. Gene Ontology (GO) and pathway analyses of differentially expressed circRNAs indicated that these identified circRNAs might play important roles in protein modification, protein binding and cellular metabolism in metastatic OMM. Functions of several selected circRNA were also identified. In addition, by using bioinformatics predictions, we further demonstrated that hsa_circ_0005320, hsa_circ_0067531 and hsa_circ_0000869 could serve as competing endogenous RNA (ceRNA), which might regulate tumorigenesis and metastatic of OMM by binding to specific microRNAs. Our results not only suggested that circRNAs might play critical roles in metastasis of OMM, but also provided critical information of circRNAs in regulating OMM progression. The findings would help us to develop potential biomarkers for clinical diagnosis and design therapeutic strategies for OMM.

Keywords: Oral mucosal melanoma, lymph nodes, metastasis, circRNA

Introduction

Oral mucosal melanoma (OMM) is an extremely rare and aggressive tumor arising from the mucosal epithelium of the oral cavity [1]. Because of its low incidence, there have been few epidemiologic and natural history studies on OMM [2]. However, OMM has relatively higher incidence in Asian that accounts for 7.5% of all melanomas, compared to less than 1% in Caucasians [3]. Previous studies have demonstrated that OMM is distinctive from cutaneous melanoma with regard to its clinical course and prognosis [4]. Most oral melanomas arise de novo from normal mucosa [5]. The definite precursor lesion has not yet been identified. The prognosis of OMM is poor. The biological behavior of OMM appears to be somehow different from that of cutaneous melanoma [6]. 5-year survival rate of OMM is only 14%, compared with 90% for cutaneous melanoma [7]. Moreover, mucosal melanomas arising from the oral cavity had a higher incidence of regional nodal dissemination and distant lung metastasis compared to cutaneous melanoma and mucosal melanomas arising from other sites (31.7% versus 19.8%, 32.5% versus 18.5%, respectively) [8]. Therefore, a better understanding of the molecular changes in OMM during tumorigenesis and metastasis would help to develop a better theraputic strategy for OMM.

CircRNAs are single-stranded, covalently closed circular molecules widely expressed across eukaryotic organisms [9], and highly stable compared to their linear types due to the resis-

tant to exonuclease [10], which makes them valuable as potential biological markers in the clinic. With recent improvements in the new generation of high-throughput sequencing and biological technologies, these molecules are shown to act as miRNA molecule sponges, which interact with RNA binding proteins and participate in gene transcriptional regulation [11]. For instance, circRNAs could negatively regulate the activity of miRNAs as miRNA sponges through competing endogenous RNA (ceRNA) networks, which compete for the miRNA response elements (MREs) to suppress gene expression [12]. Moreover, ceRNAs are implicated in the tumorigenesis of cancers when the balance of ceRNA intricate network is disturbed [13]. Previous research showed that circRNAs were differentially expressed in cutaneous melanoma cell line (WM35 and WM451) [14]. However, the role of circRNAs in OMM is unknown.

In this paper, we generated a differential expression profile of circRNAs by analysis OMMs with lymph nodes dissemination through circRNA microarray. Based on the profile, we further investigated the ceRNA networks and the potential targeting relationships of circRNAs in metastatic OMM.

Materials and methods

Patients and specimens

A total of 30 patients who were diagnosed with OMM and subjected to primary surgical treatment in the Department of Oral and Maxillofacial-Head and Neck Oncology at Shanghai Ninth People's Hospital from July 2016 to July 2017 were selected for the current study. Patients with previous histories of chemo- or radiotherapy, or with synchronous cutaneous melanoma were excluded. Fresh frozen paired tissue samples were collected from primary tumor, adjacent normal tissue and lymph nodes of each patient during the surgery. The samples were evaluated by two experienced pathologists independently. All the cases were diagnosed as OMM with synchronous cervical lymph nodes dissemination. The diagnosis of the primary tumor and metastatic lymph nodes were confirmed by immunohistochemistry. Written informed consents were obtained from all participants. The study was carried out under the ethical protocol approved by the Shanghai Ninth People's Hospital Ethical Committee.

RNA isolation

Total RNA from tumors and normal tissues were isolated by Trizol (Life Technologies, USA). Purity and quantity of isolated total RNA were determined by NanoDrop™ ND-2000 (Thermo Fisher Scientific, Scotts Valley, CA, USA). Agilent Bioanalyzer 2100 (Agilent Technologies, Santa Clara, CA, USA) was used to remove genomic DNA (gDNA) contamination and detect total RNA integrity.

Microarray analysis

Tissues from 6 primary OMM with lymph nodes dissemination were sent for circRNA microarray analysis. Sample preparation and microarray hybridization were performed according to the Arraystar's standard protocols. Total RNA from twelve samples were amplified and transcribed into fluorescent cRNA. The labeled cRNAs were hybridized and the arrays were scanned after washing the slides. The acquired array images were analyzed using the Agilent Feature Extraction software (version 11.0.1.1). circRNA was considered statistically significantly dysregulated when $FC \geq 2$ and $P < 0.05$. The microarray was performed by OE Biotechnology Company in Shanghai, People's Republic of China.

Experimental validation with RT-PCR

Hsa_circ_0005320, hsa_circ_0067531, hsa_circ_0008042, hsa_circ_0000869 and hsa_circ_0000853 were selected for experimental validation using quantitative RT-PCR. Total RNAs isolated from cancerous (primary tumor and metastatic lymph nodes) and normal tissues (paired adjacent normal tissues and normal lymph nodes) from 30 patients were subjected to reverse transcription using iScriptTMcDNA synthesis kit (Bio-Rad, CA). Quantitative PCR was performed using FastSYBR Green master mix with Rox (Life Technologies, USA) on the ABI7900HT fast real-time PCR system. The primers for circular RNAs were purchased from SABiosciences. The primer sequences were listed in Table S1. *GAPDH* was served as the control.

Bioinformatics and data analysis

GO analysis was performed to annotate genes in domains of cellular components, biological processes and molecular functions. The enrich-

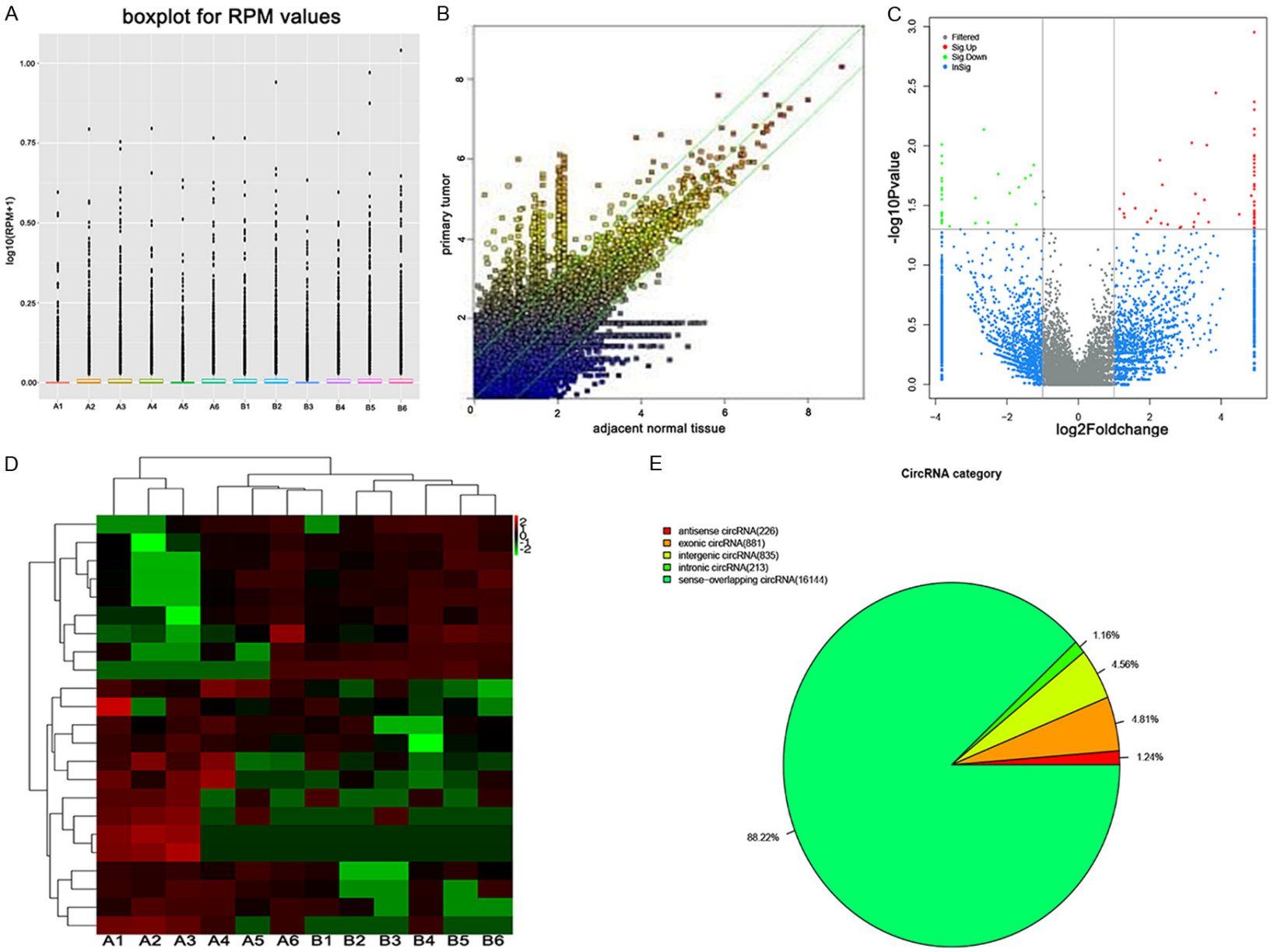
A
boxplot for RPM values
log10(RPM+1)
A1 A2 A3 A4 A5 A6 B1 B2 B3 B4 B5 B6
B
primary tumor
adjacent normal tissue
C
Fittered
Sig Up
Sig Down
InSig
-log10Pvalue
log2Foldchange
D
A1 A2 A3 A4 A5 A6 B1 B2 B3 B4 B5 B6
E
CircRNA category
antisense circRNA(226)
exonic circRNA(881)
intergenic circRNA(835)
intronic circRNA(213)
sense−overlapping circRNA(16144)
1.16%
4.56%
4.81%
1.24%
88.22%

Figure 1. A. The box plot of the distributions of circRNAs profiles. The distributions of log2 ratios among twelve samples are nearly the same after normalization. A: metastatic primary tumor; B: paired adjacent tissue. B. The scatter plot of circRNAs expressions in primary and paired adjacent tissue. X and Y axes represent the averages of normalized signal values in different groups (log2 scaled). The green lines are the fold changes. The circRNAs above the top green line and below the bottom green line are those with more than 1.5-fold change between two groups. C. Volcano plot of the differentially expressed circRNAs. The vertical lines correspond to 1.5-fold change up and down, respectively, and the horizontal line represents P = 0.05. The red point in the plot represents the differentially expressed circRNAs with statistical significance. D. Heat map and hierarchical clustering of different circRNA expression profiles in primary and paired adjacent tissue. A: metastatic primary tumor; B: paired adjacent tissue. E. Classification of dysregulated circRNAs between primary and paired adjacent tissue.

ment score calculated as the negative logarithm of *p*-value was used to determine the statistical significance of GO term clusters targeted by differentially expressed genes. KEGG analysis was used to determine the involvement of target genes in different biological pathways. Statistical significance of pathway correlations was determined by the enrichment score.

CircRNA-miRNA network analysis

It was reported that circRNAs could act as competing endogenous RNAs (ceRNA) to regulate the activities of miRNAs. Therefore, a circRNA-miRNA co-expression network (ceRNA network) was constructed by analyzing the correlations between circRNAs and miRNAs. circRNA/miRNA interactions were predicted by software miRanda. The prediction of miRNA binding sites was based on *p*-value of the hypergeometric distribution. Top 300 circRNA-miRNA interactions were selected to construct a network map by software Cytoscape.

Statistical analysis

Student's t-test was used to compare microarray and RT-PCR assay. In microarray analysis, FC ≥ 1.5 and P < 0.05 were considered statistically significant. Relative quantification of circRNA expression was evaluated using comparative CT method, and *P*-values less than 0.05 were considered significant. Data were represented as mean ± standard deviation (SD) from more than three independent experiments.

Results

Overview of circRNA expressions in the primary tumor of OMM by microarray

A microarray platform with 18,299 circRNA targets was applied to measure circRNA expression levels in six primary OMM with lymph nodes dissemination. Clinical characteristics of selected cases were listed in Table S2. The distributions of normalized circRNA intensities of the tested samples in all the datasets were virtually identical, displayed in the box plot (**Figure 1A**). The differences in circRNA expression levels between primary tumor tissue and paired adjacent normal tissue were visualized by a scatter plot. The red and green points represented the upregulated and downregulated circRNAs (FC ≥ 1.5), respectively (**Figure 1B**). Volcano plot was depicted for filtering on significantly differentially expressed circRNAs (FC ≥ 1.5 and P < 0.05) between the two groups of samples (**Figure 1C**). As a result, 90 dysregulated circRNAs in metastatic samples that fitted the criteria, FC ≥ 1.5 and P < 0.05, were identified, among which 58 were upregulated and 32 were downregulated. Top 10 differentially expressed circRNAs were listed in **Table 1**. Moreover, hierarchical clustering analysis demonstrated distinct circRNA expressions between the metastatic primary tumor and adjacent tissues (**Figure 1D**). Among all the differentially expressed circRNAs that were identified, 226 were antisense, 881 were exonic, 213 were intronic, 835 were intergenic and 16,144 were sense-overlapping circRNAs (**Figure 1E**).

Validation of selected identified dysregulated circRNAs by qRT-PCR

To further validate the microarray data, we selected five circRNAs from the top 10 dysregulated circRNAs in primary tumor and metastatic lymph nodes. The expression levels of the five circRNAs were compared between cancerous (primary tumor and metastatic nodes) and normal tissues (paired adjacent normal tissues and non-metastatic nodes) from 30 patients by RT-PCR. The results revealed that the expressions of hsa_circ_0005320, hsa_circ_0067531 and hsa_circ_0008042 were significantly upregulated in cancerous tissue compared to

Table 1. Top 10 upregulated and 8 downregulated circRNAs in the primary of OMM with lymph nodes dissemination by fold change (FC)

CircRNA ID	FC	*P* value	Type	Chromosome	Strand	Gene symbol
hsa_circ_0005320	22.6049	0.037153	Exonic	NC_000017.11	+	SEPT9
hsa_circ_0008558	14.4722	0.003589	Sense-overlapping	NC_000016.10	+	LONP2
hsa_circ_0067531	12.1204	0.00988	Sense-overlapping	NC_000003.12	-	PIK3CB
hsa_circ_0008042	11.5061	0.028256	Sense-overlapping	NC_000005.10	+	CPEB4
hsa_circ_0062321	10.3088	0.036896	Sense-overlapping	NC_000022.11	-	KLHL22
hsa_circ_0001554	9.68497	0.025186	Sense-overlapping	NC_000005.10	+	RANBP17
hsa_circ_0030507	9.36722	0.047737	Sense-overlapping	NC_000013.11	-	MYCBP2
hsa_circ_0003192	9.02056	0.009422	Sense-overlapping	NC_000002.12	-	WDR33
hsa_circ_0002510	7.29596	0.047321	Sense-overlapping	NC_000012.12	-	SBNO1
hsa_circ_0017648	4.99816	0.044273	Sense-overlapping	NC_000010.11	-	SFMBT2
hsa_circ_0000869	-4.75238	0.017108	Intronic	NC_000019.10	-	GNG7
hsa_circ_0006733	-5.74527	0.044015	Sense-overlapping	NC_000018.10	-	ROCK1
hsa_circ_0025908	-6.28837	0.007245	Sense-overlapping	NC_000012.12	+	PPHLN1
hsa_circ_0018900	-7.39479	0.044556	Sense-overlapping	NC_000010.11	+	ADK
hsa_circ_0057041	-10.309	0.001794	Sense-overlapping	NC_000002.12	-	METTL8
hsa_circ_0001062	-2.28529	0.030688	Exonic	NC_000002.12	+	ZC3H6
hsa_circ_0000853	-2.39373	0.014384	Sense-overlapping	NC_000018.10	+	MALT1
hsa_circ_0000596	-2.51585	0.017477	Sense-overlapping	NC_000015.10	+	CASC4

CircRNA ID was based on circBase (http://www.circbase.org/).

paired normal tissues, whereas the expressions of hsa_circ_0000869 and hsa_circ_0000853 were significantly downregulated (**Figure 2**). Our qRT-PCR data verified the results of microarray. circRNAs expressions were not only dysregulated in lymph nodes but also in the primary tumor. The findings provided valid evidence that these circRNAs might be associated with the metastasis process of OMM.

Distributions of differentially expressed circRNAs in the primary OMM

We categorized the identified circRNAs based on the chromosomes they were transcribed from, and found that these circRNAs were distributed equally among all chromosomes, including sex chromosomes. The top five chromosomes that transcribe dysregulated circRNAs in the metastatic tissues were chromosome1 (chr1, 1,783 transcripts, 9.7%), chr2 (1,674 transcripts, 9.1%), chr3 (1,254 transcripts, 6.9%), chr11 (1,063 transcripts, 5.8%), and chr5 (1,000 transcripts, 5.5%) (**Figure 3A**). We also compared our circRNAs datasets with circBase and found that 8,878 circRNAs were overlapped with the public database (**Figure 3B**).

GO and pathway analyses

In order to explore how circRNAs regulate parental gene expression, GO analysis was performed to annotate genes targeted by the differentially expressed circRNAs in domains of biological processes, cellular components and molecular functions. Gene expression profile of linear counterparts of differentially expressed circRNAs in metastatic tissues suggested their potential roles in protein modification, protein binding and cellular protein metabolism (**Figure 3C**). According to the results, protein N-linked glycosylation via asparagine (GO: 0018279, P = 5.13 E-06), Golgi membrane in the cellular component (GO: 0000139, P = 2.73 E-03), and peptidase activity in the molecular function (GO: 0004197, P = 5.67 E-06) were the top annotation cluster terms of the biological processes (**Figure 3C**). Upregulated and downregulated circRNAs ($P < 0.05$) were shown in **Figure 3D** and **3E**, respectively. Finally, KEGG pathway enrichment analysis indicated that 6 pathways involved in metastasis were associated with the dysregulated circRNAs (**Figure 3F**), suggesting that these pathways might significantly contribute to the tumor progression of OMM. With regard to the specific biological functions relat-

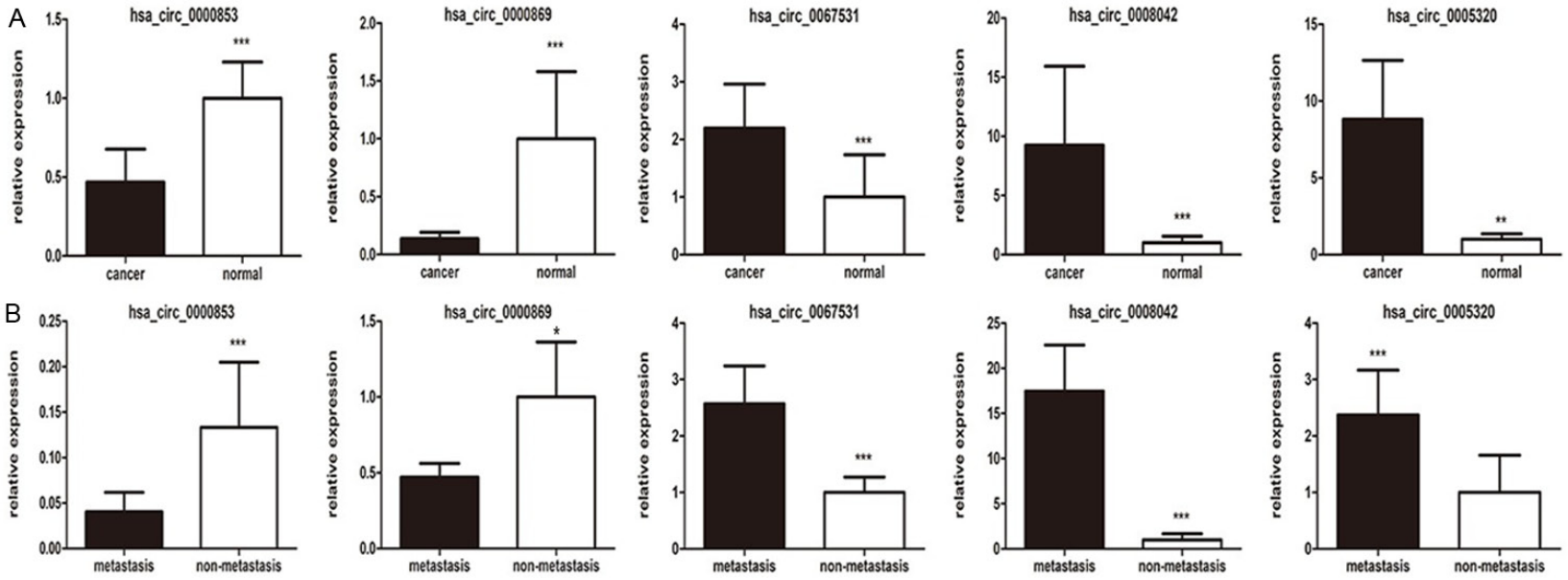

Figure 2. A. Expressions of hsa_circ_0005320, hsa_circ_0067531, hsa_circ_0008042, hsa_circ_0000869 and hsa_circ_0000853 in primary and adjacent normal tissues (n = 30). B. Expressions of hsa_circ_0005320, hsa_circ_0067531, hsa_circ_0008042, hsa_circ_0000869 and hsa_circ_0000853 in metastatic and paired non-metastatic lymph nodes (n = 30). Each bar represents the average logarithm of circRNAs expression level to the base 2 (log2 (x)), *P*-values were calculated by Wilcoxon rank-sum test. (**P < 0.05, t-test).

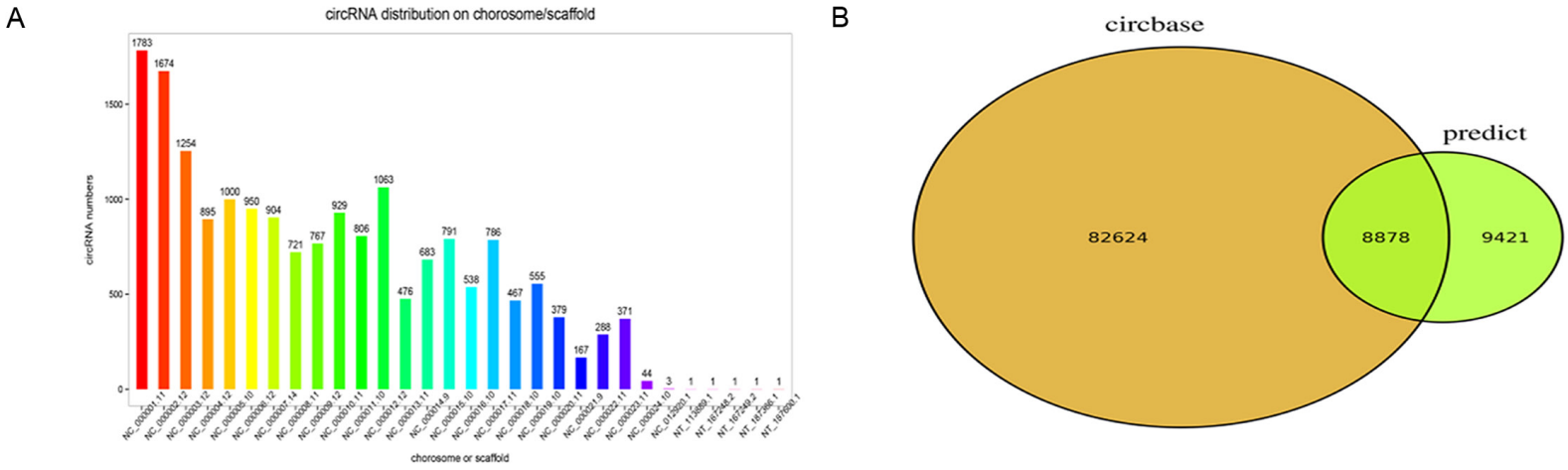

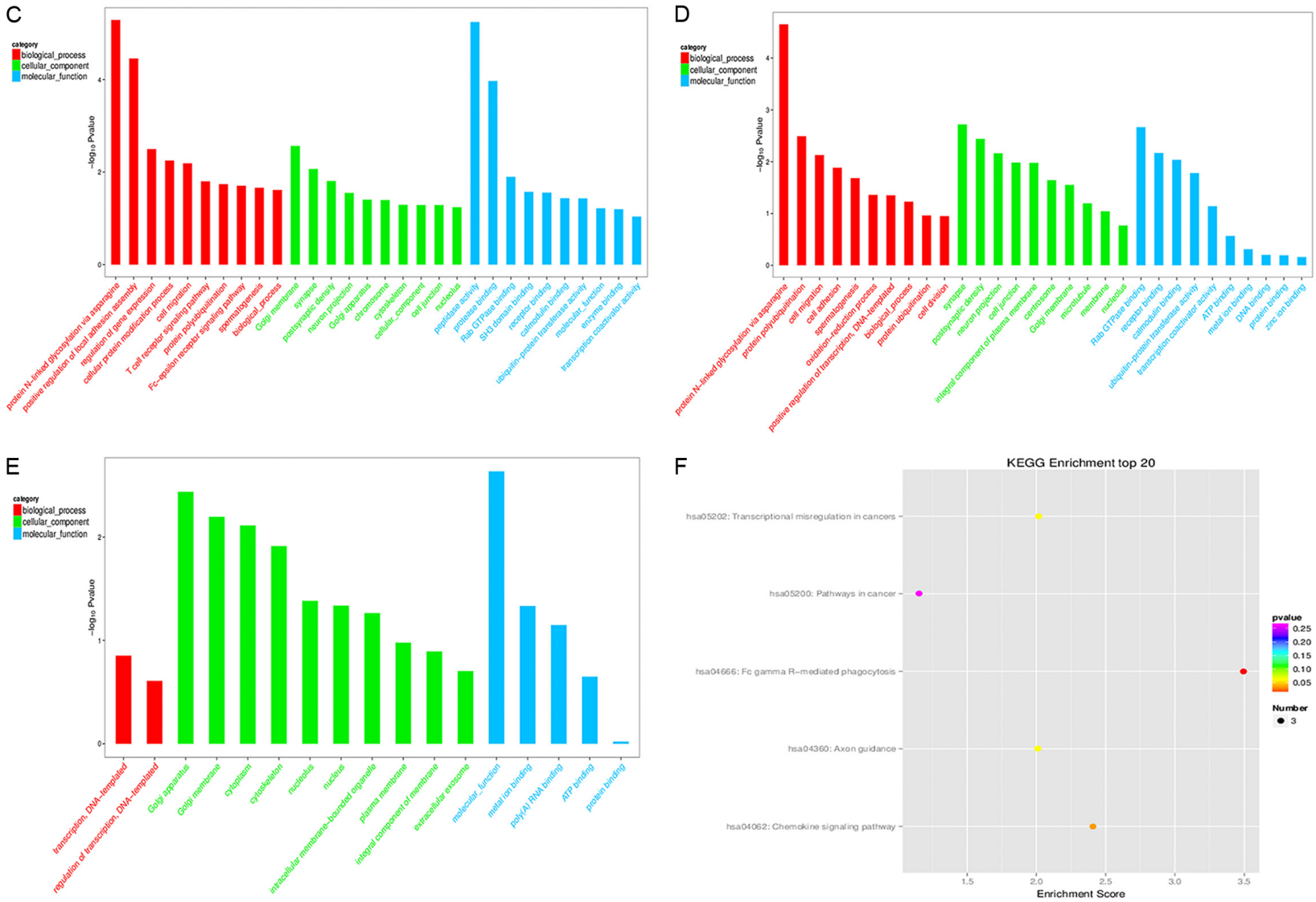

Figure 3. A. The distribution of dysregulated circRNAs in chromosomes. B. The comparison of our predicted circRNAs datasets with circRNAs public database (circBase) using software CIRI. C. Most significantly enriched GO terms (-log10 (*P* value)) of circRNAs gene symbols in domains of biological processes, cellular components and molecular functions. D. Most significantly enriched GO terms (-log10 (*P* value)) of up-regulated circRNAs gene symbols in domains of biological processes, cellular components and molecular functions. E. Most significantly enriched GO terms (-log10 (*P* value)) of down-regulated circRNAs gene symbols in domains of biological processes, cellular components and molecular functions. F. The bar plot depicts the enrichment score (-log10 (*P* value)) of significantly enriched pathways.

Table 2. GO terms of the selected 5 circRNAs

CircRNA ID	GO ID	GO terms
hsa_circ_0005320	GO: 0003924, GO: 0005525, GO: 0031105	GTPase activity, GTP binding, septin complex
hsa_circ_0067531	GO: 0000187, GO: 0005524	Activation of MAPK activity, ATP binding
hsa_circ_0008042	GO: 0000166, GO: 0000900, GO: 0005634	Nucleotide binding, translation repressor activity, nucleic acid binding nucleus
hsa_circ_0000869	GO: 0007186, GO: 0008277	G-protein coupled receptor signaling pathway, regulation of G-protein coupled receptor protein signaling pathway
hsa_circ_0000853	GO: 0001923, GO: 0051168	Activation of NF-kappa B-inducing kinase activity, positive regulation of I-kappa B kinase/NF-kappa B signaling

ed to our selected circRNAs, hsa_circ_0005320 was associated with GTPase activity (GO: 0003924); hsa_circ_0067531 was related with activation of MAPK activity (GO: 0000187); hsa_circ_0008042 played a potential role in translation repressor activity (GO: 0000900); hsa_circ_0000869 might be involved in G-protein coupled receptor (GPR) signaling pathway (GO: 0007186) and hsa_circ_0000853 might be involved in NF-kappa B signaling pathway (GO: 0001923) (**Table 2**).

*Prediction of miRNAs targeted by differentially expressed circRNA*s

CircRNAs can post-transcriptionally regulate the expression of genes by serving as ceRNAs and regulate miRNA response elements. To explore the possible interactions between miRNA and circRNA, we constructed a ceRNA network map that showed the co-expression pattern of circRNA-miRNA. The expression profiles were based on the high-throughput sequencing data. Top 300 interactions between circRNAs and miRNAs ranked by the *p*-value of the hypergeometric distribution were shown in **Figure 4**. MiRNAs that were significantly correlated with the selected circRNAs were shown in **Table 3**, and three selected circRNAs (hsa_circ_0005320, hsa_circ_0067531 and hsa_circ_0000869) were annotated in detail to predict the potential miRNA binding sites (**Figure 5A**) and correlation with their potential mRNA targets (**Figure 5C**) using the circRNA/miRNA interaction information. Specific parameters of correlation with potential mRNA targets were shown in Table S3. Then we performed receiver operating characteristic (ROC) curve analysis to test the diagnostic potential of our selected circRNAs in OMM patients, the AUC values were 0.889 in hsa_circ_0000869, 0.833 in hsa_circ_0005320 and 0.889 in hsa_circ_0067531 respectively (**Figure 5B**), indicating the high diagnostic potential of our selected circRNAs. Taken together, the results provided us a novel perspective to explore the underlying mechanisms of circRNAs that contribute to the tumorigenesis and/or development of OMM.

Discussion

CircRNAs are derived from splicing errors with low abundance [15]. Nevertheless, emerging evidences indicate that circRNAs belong to a large category of highly stable non-coding RNAs (ncRNAs) that has no protein coding function and serves as pivotal gene regulators for transcription and translation [16]. CircRNAs may come from intronic and/or exonic sequences. They can act as miRNA sponges, splicing and transcription regulators that modify parental gene expressions [17]. Recent studies have correlated the dysregulation of circRNA expression with various malignant neoplasms by high-throughput RNA sequencing and bioinformatics analyses [18], suggesting that circRNAs might have potentials to become ideal biomarkers for cancers.

This paper is the first report on the investigation of circRNAs expression profiles in metastatic OMM. In the study, we systematically searched for head-to-tail backsplicing junctions among annotations of exons, and identified thousands of circRNA candidates in six primary OMM with lymph nodes dissemination. The microarray expression profiles revealed that 58 circRNAs were significantly upregulated and 32

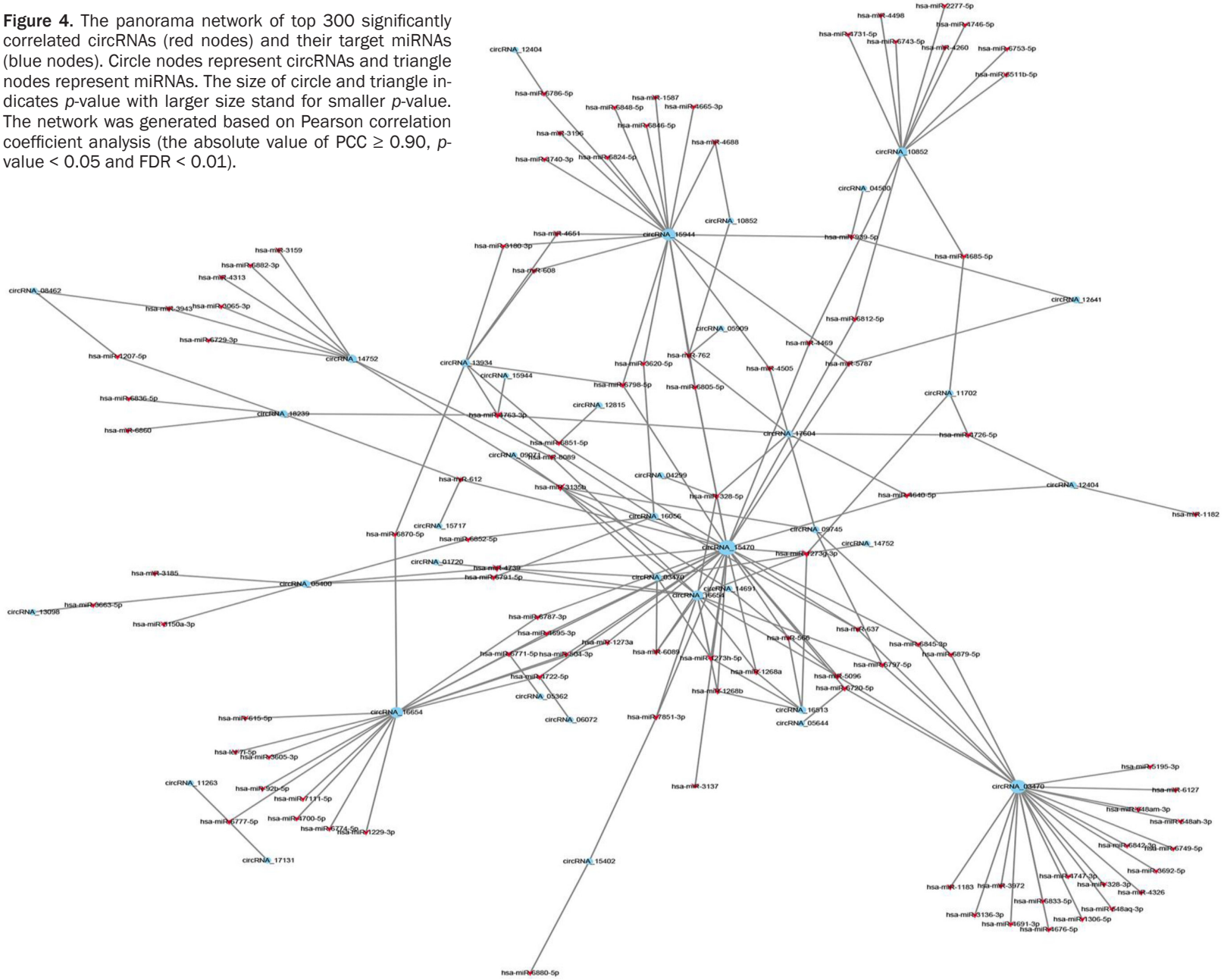

Figure 4. The panorama network of top 300 significantly correlated circRNAs (red nodes) and their target miRNAs (blue nodes). Circle nodes represent circRNAs and triangle nodes represent miRNAs. The size of circle and triangle indicates *p*-value with larger size stand for smaller *p*-value. The network was generated based on Pearson correlation coefficient analysis (the absolute value of PCC ≥ 0.90, *p*-value < 0.05 and FDR < 0.01).

Table 3. Potential miRNA targets of dysregulated circRNAs

CircRNA ID	Regulation	Gene symbol	Potential miRNA targets
hsa_circ_0005320	Up	SEPT9	miR-4740-3p; miR-4505; miR-6786-5p; miR-6805-5p; miR-3180-3p; miR-4665-3p; miR-3196; miR-6798-5p; miR-4688; miR-939-5p; miR-762; miR-6824-5p; miR-4763-3p; miR-608; miR-4651; miR-1587; miR-6846-5p; miR-3620-5p; miR-5787; miR-6848-5p
hsa_circ_0067531	Up	PIK3CB	miR-328-5p
hsa_circ_0000869	Down	GNG7	miR-1268a; miR-1268b; miR-566; miR-1273h-5p; miR-1273g-3p

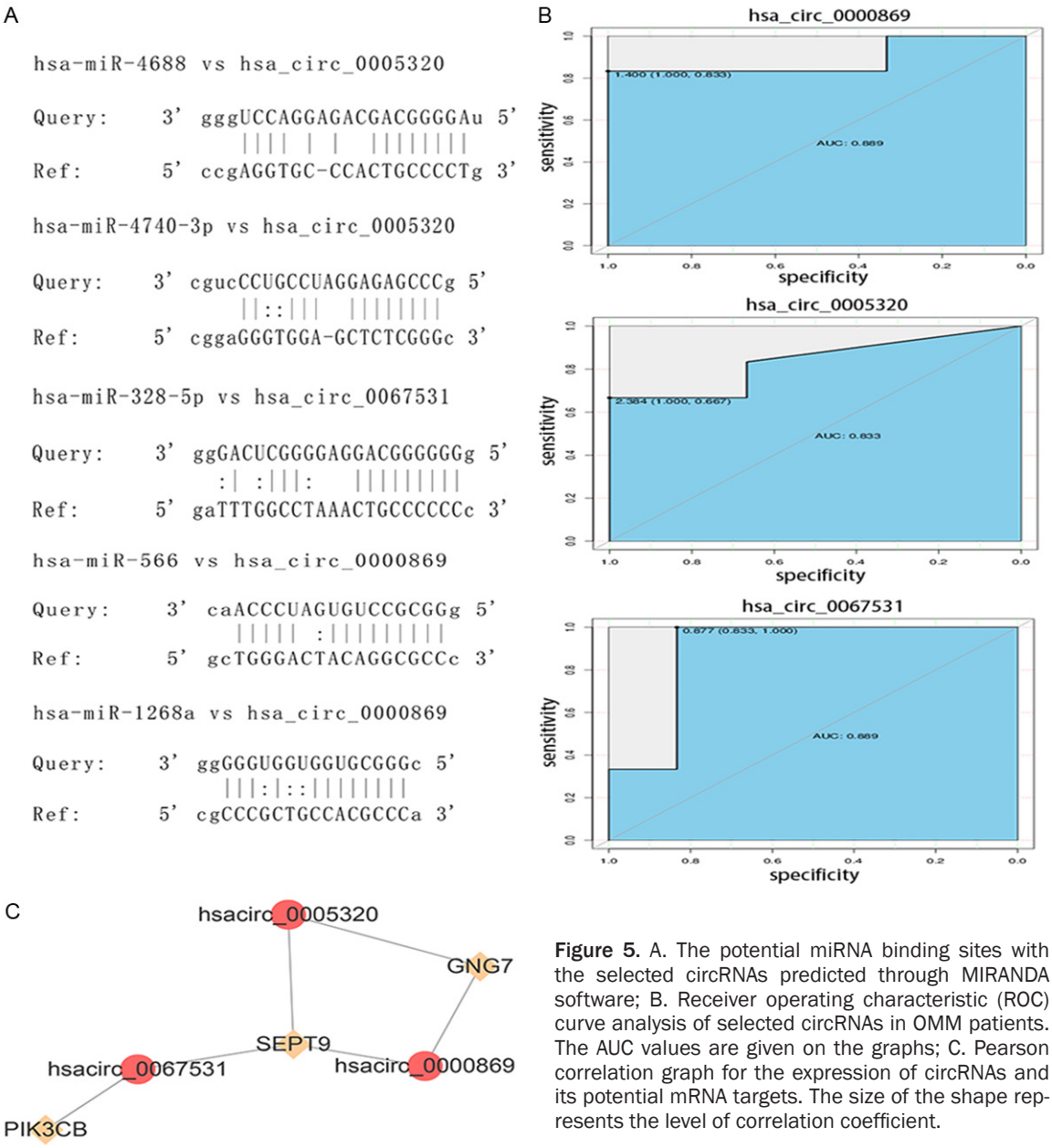

Figure 5. A. The potential miRNA binding sites with the selected circRNAs predicted through MIRANDA software; B. Receiver operating characteristic (ROC) curve analysis of selected circRNAs in OMM patients. The AUC values are given on the graphs; C. Pearson correlation graph for the expression of circRNAs and its potential mRNA targets. The size of the shape represents the level of correlation coefficient.

circRNAs were significantly downregulated. The function of most identified dysregulated circRNAs were homologous, suggesting that these circRNAs might contribute to the pathogenesis of OMM. In particular, our results indicated that the expressions of hsa_circ_0005320, hsa_

circ_0067531 and hsa_circ_0008042 were significantly upregulated in both primary tumor and metastatic lymph nodes compared with those in adjacent and non-metastatic tissues. Hsa_circ_0005320, encoded by SEPT9, belongs to the septin gene family that plays important roles in cytokinesis and cell cycle control. Studies have shown that this gene is a potential tumor suppressor that may inhibit the invasion of ovarian cancer [19]. Hsa_circ_0067531 is spliced from PIK3CB, which encodes an isoform of the phosphoinositide 3-kinase catalytic subunit. PIK3CB is critical in triggering cancer-related signaling pathways. Inhibition of PIK3CB could increase the sensitivity of BRAF kinase inhibitors in melanoma, although BRAF mutations are rare (less than 10%) in OMM [20]. Hsa_circ_0008042 is derived from gene MYCBP2, which could help melanoma cells progress through G1/S cell cycle checkpoints and promote cell proliferation [21]. Conversely, hsa_circ_0000869 and hsa_circ_0000853 were significantly downregulated in both primary tumor and disseminated lymph nodes. Hsa_circ_0000869 is spliced from GNG7, a gene associated with autophagy and the inhibition of cell division [22] Hsa_circ_0000853 is encoded by MALT1. MALT1 is frequently rearranged in chromosomal translocation in mucosa-associated lymphoid tissue lymphomas, and involved in biological processes like NF-kappa B activation and regulation of cancer cell proliferation and migration [23].

GO analysis demonstrated that the differentially expressed genes were enriched in biological processes including protein association, modification and regulation of cellular metabolism. Among the GO terms identified in this study, FUT protein glycosylation complex has been proved in playing a crucial role in promoting OMM metastasis [24]. In addition, N-Glycan biosynthesis signaling pathway has been reported to be involved in the progression of OMM [25]. As for our selected circRNAs, hsa_circ_0067531 was related to the activation of MAPK, and hsa_circ_0000853 might be involved in MAPK and NF-kappa B signaling pathways that are reported to play critical roles in promoting melanoma metastases [26]. It has been shown that G-protein-coupled receptor 120 (GPR120) could serve as a novel biomarker for melanoma metastasis [27]. We found that hsa_circ_0000869 might be involved in GPR signaling pathway, indicating that hsa_circ_0000869 may regulate OMM metastasis through GPRs. Together, our findings indicated that certain circRNAs might be involved in the metastasis and progression of OMM through modulating several cancer related signaling pathways, including protein N-glycosylation.

Studies have shown that sponging miRNAs (i.e. ceRNA) have an impact on oncogenesis and cancer progression through the regulation of gene expression at post-transcriptional level via circRNA-miRNA-mRNA regulatory axes [28]. Seeking potential miRNA targets of circRNAs using the miRNA target predication software in order to construct interaction networks, we were able to identify several possible cancer-related pathways based on sequence pairing to the predicted circRNA-miRNA-mRNA regulatory axes. This information is very important for understanding the mechanisms that underlying the action of circRNAs in metastatic OMM. For instance, emerging evidence indicated that dysregulated miR-1228-5p could serve as a potential biomarker for hepatocellular carcinoma (HCC) because it was associated with cellular apoptosis through a mitochondria-dependent pathway [29]. Furthermore, miR-1268a was reported to be a potential risk factor and prognostic biomarker for AFB1-related HCC, and low miR-1268a expression may be beneficial for post-operative adjuvant TACE treatment in HCC [30]. Our data demonstrated that hsa_circ_0032249 could potentially bind to miR-1228-5p, and hsa_circ_0000869 contained multiple binding sites for miR-1268a, indicating that hsa_circ_0032249 and hsa_circ_0000869 could regulate miRNAs function by serving as ceRNAs, which might contribute to the development and progression of OMM.

In conclusion, we have demonstrated that numerous circRNAs were dysregulated in OMM for the first time. The aberrantly expressed circRNAs may be potentially involved in the progression and metastasis of OMM and might serve as potential diagnostic biomarkers for OMM. Given that a single circRNA could regulate various downstream genes via a common microRNA target, our observation suggested that these circRNAs might potentially act as cancer drivers through highly enriched signaling pathways. Despite that the possibility of obtaining false positive results when evaluating

circRNA expression could exist due to the relatively low expression levels of circRNAs and the detection thresholds used in current study, our results provided new exciting information that would not only help researchers uncover the complex biological functions of circRNAs involved in the carcinogenesis of OMM, but also provided evidences that circRNAs could serve as potential diagnostic and/or prognostic markers for OMM.

Acknowledgements

This study was supported by grants from the National Program on Key Research Project of China (2016YFC0902700), National Natural Science Foundation of China (No. 31140007, 81472516) and the project of Science and Technology Commission of Shanghai Municipality (Grant #14DZ1941402).

Disclosure of conflict of interest

None.

Address correspondence to: Guoxin Ren, Min Ruan and Jingzhou Hu, Department of Oral Maxillofacial-Head and Neck Oncology, Shanghai Ninth People's Hospital, School of Medicine, Shanghai Jiao Tong University, 639 Zhi-Zao-Ju Road, Shanghai 200011, China. Tel: 86-21-23271699-5658; E-mail: renguoxincn@sina.com (GXR); doctorruanmin@hotmail.com (MR); huyayi@shsmu.edu.cn (JZH)

References

[1] Chatzistefanou I, Kolokythas A, Vahtsevanos K, Antoniades K. Primary mucosal melanoma of the oral cavity: current therapy and future directions. Oral Surg Oral Med Oral Pathol Oral Radiol 2016; 122: 17-27.

[2] Mikkelsen LH, Larsen AC, von Buchwald C, Drzewiecki KT, Prause JU, Heegaard S. Mucosal malignant melanoma - a clinical, oncological, pathological and genetic survey. APMIS 2016; 124: 475-486.

[3] Wushou A and Zhao YJ. The management and site-specific prognostic factors of primary oral mucosal malignant melanoma. J Craniofac Surg 2015; 26: 430-434.

[4] Furney SJ, Turajlic S, Stamp G, Nohadani M, Carlisle A, Thomas JM, Hayes A, Strauss D, Gore M, van den Oord J, Larkin J, Marais R. Genome sequencing of mucosal melanomas reveals that they are driven by distinct mechanisms from cutaneous melanoma. J Pathol 2013; 230: 261-269.

[5] Meleti M, Leemans CR, Mooi WJ, Vescovi P, van der Waal I. Oral malignant melanoma: a review of the literature. Oral Oncol 2007; 43: 116-121.

[6] Alaeddini M and Etemad-Moghadam S. Immunohistochemical profile of oral mucosal and head and neck cutaneous melanoma. J Oral Pathol Med 2015; 44: 234-238.

[7] Breik O, Sim F, Wong T, Nastri A, Iseli TA, Wiesenfeld D. Survival outcomes of mucosal melanoma in the head and neck: case series and review of current treatment guidelines. J Oral Maxillofac Surg 2016; 74: 1859-1871.

[8] Lian B, Cui CL, Zhou L, Song X, Zhang XS, Wu D, Si L, Chi ZH, Sheng XN, Mao LL, Wang X, Tang BX, Yan XQ, Kong Y, Dai J, Li SM, Bai X, Zheng N, Balch CM, Guo J. The natural history and patterns of metastases from mucosal melanoma: an analysis of 706 prospectively-followed patients. Ann Oncol 2017; 28: 868-873.

[9] Jeck WR, Sorrentino JA, Wang K, Slevin MK, Burd CE, Liu J, Marzluff WF, Sharpless NE. Circular RNAs are abundant, conserved, and associated with ALU repeats. RNA 2013; 19: 141-157.

[10] Chen LL. The biogenesis and emerging roles of circular RNAs. Nat Rev Mol Cell Biol 2016; 17: 205-211.

[11] Hansen TB, Jensen TI, Clausen BH, Bramsen JB, Finsen B, Damgaard CK, Kjems J. Natural RNA circles function as efficient microRNA sponges. Nature 2013; 495: 384-388

[12] Ferdin J, Kunej T and Calin GA. Non-coding RNAs: identification of cancer-associated microRNAs by gene profiling. Technol Cancer Res Treat 2010; 9:123-138.

[13] Lee Y, Ahn C, Han J, Choi H, Kim J, Yim J, Lee J, Provost P, Rådmark O, Kim S, Kim VN. The nuclear RNase III Drosha initiates microRNA processing. Nature 2003; 425: 415-419.

[14] Wang Q, Chen J, Wang A, Sun L, Qian L, Zhou X, Liu Y, Tang S, Chen X, Cheng Y, Cao K, Zhou J. Differentially expressed circRNAs in melanocytes and melanoma cells and their effect on cell proliferation and invasion. Oncol Rep 2018; 39: 1813-1824.

[15] Robinson MD, Mccarthy DJ and Smyth GK. edgeR: a Bioconductor package for differential expression analysis of digital gene expression data. Bioinformatics 2010; 26: 139-140.

[16] Qu S, Zhong Y, Shang R, Zhang X, Song W, Kjems J, Li H. The emerging landscape of circular RNA in life processes. RNA Biol 2016; 14: 1-8.

[17] Sand M, Bechara FG, Gambichler T, Sand D, Bromba M, Hahn SA, Stockfleth E, Hessam S. Circular RNA expression in cutaneous squamous cell carcinoma. J Dermatol Sci 2016; 83: 210-218.

[18] Qu S, Yang X, Li X, Wang J, Gao Y, Shang R, Sun W, Dou K, Li H. Circular RNA: a new star of noncoding RNAs. Cancer Lett 2015; 365: 141-148.
[19] Huang YS, Jie N, Zou KJ, Weng Y. Expression profile of circular RNAs in human gastric cancer tissues. Mol Med Rep 2017; 16: 2469-2476.
[20] Scott M, McCluggage WG, Hillan KJ, Hall PA, Russell SE. Altered patterns of transcription of the septin gene, SEPT9, in ovarian tumorigenesis. Int J Cancer 2006; 118: 1325-1329.
[21] Bonnevaux H, Lemaitre O, Vincent L, Levit MN, Windenberger F, Halley F, Delorme C, Lengauer C, Garcia-Echeverria C, Virone-Oddos A. Concomitant inhibition of PI3Kbeta and BRAF or MEK in PTEN-Deficient/BRAF-mutant melanoma treatment: preclinical assessment of SAR260301 oral PI3Kbeta-selective inhibitor. Mol Cancer Ther 2016; 15: 1460-1471.
[22] Pérez-Guijarro E, Karras P, Cifdaloz M, Martínez-Herranz R, Cañón E, Graña O, Horcajada-Reales C, Alonso-Curbelo D, Calvo TG, Gómez-López G, Bellora N, Riveiro-Falkenbach E, Ortiz-Romero PL, Rodríguez-Peralto JL, Maestre L, Roncador G, de Agustín Asensio JC, Goding CR, Eyras E, Megías D, Méndez R, Soengas MS. Lineage-specific roles of the cytoplasmic polyadenylation factor CPEB4 in the regulation of melanoma drivers. Nat Commun 2016; 7: 13418.
[23] Liu J, Ji X, Li Z, Yang X, Wang W, Zhang X. Protein gamma subunit 7 induces autophagy and inhibits cell division. Oncotarget 2016; 7: 24832-24847.
[24] Yang F, Liu X, Liu Y, Liu Y, Zhang C, Wang Z, Jiang T, Wang Y. miR-181d/MALT1 regulatory axis attenuates mesenchymal phenotype through NF-kappa B pathways in glioblastoma. Cancer Lett 2017; 396: 1-9.
[25] Agrawal P, Fontanals-Cirera B, Sokolova E, Jacob S, Vaiana CA, Argibay D, Davalos V, McDermott M, Nayak S, Darvishian F, Castillo M, Ueberheide B, Osman I, Fenyö D, Mahal LK, Hernando E. A systems biology approach identifies FUT8 as a driver of melanoma metastasis. Cancer Cell 2017; 31: 804-819, e807.
[26] Kunz M and Holzel M. The impact of melanoma genetics on treatment response and resistance in clinical and experimental studies. Cancer Metastasis Rev 2017; 36: 53-75.
[27] Kleemann J, Hrgovic I, Ter-Nedden J, Kleimann P, Steinhorst K, Härle K, Müller J, Kaufmann R, Meissner M, Kippenberger S. Fatty acid receptor GPR120: a novel marker for human melanoma. Melanoma Res 2018; 4: 271-276.
[28] Huang M, Zhong Z, Lv M, Shu J, Tian Q, Chen J. Comprehensive analysis of differentially expressed profiles of lncRNAs and circRNAs with associated co-expression and ceRNA networks in bladder carcinoma. Oncotarget 2016; 7: 47186-47200.
[29] Tan Y, Ge G, Pan T, Wen D, Chen L, Yu X, Zhou X, Gan J. A serum microRNA panel as potential biomarkers for hepatocellular carcinoma related with hepatitis B virus. PLoS One 2014; 9: e107986.
[30] Chen X, Lu P, Wang DD, Yang SJ, Wu Y, Shen HY, Zhong SL, Zhao JH, Tang JH. The role of miRNAs in drug resistance and prognosis of breast cancer formalin-fixed paraffin-embedded tissues. Gene 2016; 595: 221-226.

Table S1. The primer sequences of the selected 5 circRNAs

circRNA	Forward Primer (5' → 3')	Reverse Primer (5' → 3')
hsa_circ_0005320	AGATGCCCAAGCCTGCTGAG	TGTCTCGACCTCCTCGACCT
hsa_circ_0067531	TAGGCTGCCTGCGACAGATG	CGGCAGTCTTGTCGCAAAGT
hsa_circ_0008042	AAGGAGCTGGGAGAGTTGCG	TGATCCCCACGGCCATCATC
hsa_circ_0000869	TACAGGCATGAACCACCGCA	CGGGAGTCAATGGCATGTGG
hsa_circ_0000853	TTCAGCCAGTGGTCACAGCT	TTGCCCGGCAACACAGTTTC

Table S2. Clinical and histopathological characteristics of patients for circRNAs assay

Patient ID	Age	Gender	TNM stage	Anatomic site
1	65	Male	cT4N2M0	Palate
2	50	Male	cT4N1M0	Gingiva
3	57	Female	cT4N2M0	Gingiva
4	64	Female	cT4N1M0	Gingiva
5	34	Male	cT4N1M0	Gingiva
6	63	Male	cT4N1M0	Palate

Table S3. Specific parameters of Pearson correlation for the expression of circRNAs and its potential mRNA targets

circRNA id	Transcript id	Gene	Correlation coefficient	*p*-value
hsacirc_0005320	NM_001293695.1	Sept-9	0.921	2.10 E-05
hsacirc_0005320	NM_006640.4	Sept-9	0.895	8.22 E-05
hsacirc_0005320	NM_001113492.1	Sept-9	0.894	8.80 E-05
hsacirc_0005320	NM_001113491.1	Sept-9	0.885	0.0001
hsacirc_0005320	XM_011524206.1	Sept-9	0.758	0.0043
hsacirc_0005320	NM_001293698.1	Sept-9	-0.750	0.0049
hsacirc_0000869	NM_052847.2	GNG7	0.694	0.0122
hsacirc_0067531	XM_006713659.2	PIK3CB	0.683	0.0144
hsacirc_0005320	NM_001113494.1	Sept-9	0.670	0.0172
hsacirc_0005320	NM_001113493.1	Sept-9	-0.661	0.0192
hsacirc_0067531	NM_001113493.1	Sept-9	-0.651	0.0220
hsacirc_0005320	NM_052847.2	GNG7	-0.650	0.0221
hsacirc_0000869	XM_011524208.1	Sept-9	0.634	0.0270
hsacirc_0067531	NM_001256045.1	PIK3CB	0.610	0.0351